Mon. Not. R. Astron. Soc. **000**, 000–000 (0000) Printed 1 February 2008 (MN LATEX style file v1.4)

THE MORPHOLOGY OF HII GALAXIES

Eduardo Telles[1,2⋆]
Jorge Melnick[3]
Roberto Terlevich[2]

1. Institute of Astronomy, Madingley Road, Cambridge CB3 0HA, U.K.
2. Royal Greenwich Observatory, Madingley Road, Cambridge CB3 0EZ, U.K.
3. European Southern Observatory, La Silla, Chile
etelles@cosmos.iagusp.usp.br, jmelnick@eso.org & rjt@ast.cam.ac.uk

arXiv:astro-ph/9701062v1 13 Jan 1997

accepted January 7, 1997

ABSTRACT

We present CCD images of a sample of 39 HII galaxies taken at the Danish 1.54m telescope on La Silla. The images are used to analyse the morphology of these emission line dwarfs, and the structural properties of the knots of star formation and of the underlying galaxy. The sizes of the starbursts are measured. We propose a morphological classification based on the presence or absence of signs of tails, extensions, or distorted outer isophotes. This criterion segregates the objects into two broad morphological types with different physical properties: the more disturbed and extended (type I) HII galaxies having larger luminosities and velocity dispersions than the more compact and regular (type II) objects. The relative position of HII galaxies and of a sample of dwarf elliptical galaxies in the [R – σ] diagram support the hypothesis of a possible evolutionary link between the two types of galaxy.

Key words: HII region – galaxies: dwarf – galaxies: starburst – galaxies: structure.

1 INTRODUCTION

HII galaxies are narrow emission line dwarf galaxies undergoing violent star formation (Melnick, Terlevich & Eggleton 1985) whose spectroscopic properties are indistinguishable from extragalactic giant HII regions in normal late type galaxies (e.g. 30 Dor in LMC, NGC 604 in M33) (Sargent & Searle 1970). Their high rates of star formation and low heavy element abundances imply that the star formation history must be simple and episodic (i.e. few burst of short duration followed by long quiescent periods). A recent review on the global properties of HII galaxies is given by Telles (1995, and references therein). The possible links of HII galaxies with other types of known dwarf galaxies have been discussed by Thuan (1983); Loose & Thuan (1985); Bothun et al. (1986); Kunth, Maurogordato & Vigroux (1988); Davies & Phillipps (1988), Drinkwater & Hardy (1991). However, no conclusive answer has been given to the questions of what these systems will resemble when the present period of violent star formation ends, or what triggered the burst. It has been suggested that in their quiescent phase HII galaxies may be related to dwarf irregulars (dI) or dwarf elliptical galaxies (dE). Bothun et al. (1986) made a comparative study of dIs and dEs in the Virgo cluster based on the colour distributions and structural properties derived from exponential fits to the surface brightness profiles (e.g. scale length and central brightness). They conclude that dIs are not progenitors of dEs, but they seem to form a parallel sequence of dwarf galaxies. The fading of dIs would make them very diffuse and place them below the detection threshold of photographic plates. They propose that Blue Compact Galaxies (BCG's, of which HII galaxies are a subset) could probably be gas-rich analog of dEs. Meurer, Mackie & Carignan (1994) have studied the structural properties of the dwarf amorphous galaxy NGC 2915 and compared with the properties of NGC 1705 (Meurer, Freeman & Dopita 1992) and NGC 5253 from the work of and Sérsic & Donzelli (1992). They find that their luminosity profiles show two components indicating the presence of two distinct stellar populations. The inner component represents the fraction of the galaxy dominated by hydrogen gas photoionized by the embedded massive star clusters. Its (B-R) colour profile is increasingly bluer inwards. The outer component has an exponential luminosity (also found for dE's and dIrr's) and a constant redder colour likely to represent

⋆ present address: Instituto Astronômico e Geofísico - USP, Caixa Postal 9638, 01065-970 - São Paulo - BRASIL

© 0000 RAS

an old stellar population remnant from a previous burst of star formation. Their main conclusion is that these galaxies are nearby BCG's that may provide a better insight on the properties of this type of galaxy and their connection with other dwarf galaxies. Kunth, Maurogordato & Vigroux (1988) analysed a small sample of BCG's to derive surface brightness profiles by ellipse fitting to different isophotal levels. Their results show that the BCG's present a "mixed bag of morphologies". They find that the outer parts of the galaxies can be best fitted by a power law compared with those of elliptical galaxies.

No definitive study has been made on the morphology of HII galaxies (or BCG's for that matter) up to now. The previous attempts have shown an extensive range of shapes from the most compact and apparently isolated to some clearly revealing diffuse extensions, multiple tails, and visually merging systems (Loose & Thuan 1985; Melnick 1987; Kunth, Maurogordato & Vigroux 1988; Salzer, MacAlpine & Boroson 1989b). Loose & Thuan (1985) have devised a classification scheme based on the shape and location of the burst in relation with the whole optical structure and the shapes of the outer envelopes. Melnick (1987) describes the systems in terms of being interacting, multiple, or isolated. He has preliminarily reported that 50% of the HII galaxies in his sample are star-like and isolated. Salzer, MacAlpine & Boroson (1989b), on the other hand, adopted a more detailed classification scheme. Primarily based on the absolute magnitude, size, and morphology, with some spectroscopic information as a secondary indicator, they identified 10 different classes of objects for a sample of emission line objects from the University of Michigan (UM) objective prism survey. Their sample includes some Seyfert galaxies as well as interacting pairs of disk galaxies, starburst nuclei and giant irregulars. Most HII galaxies in our sample are classified as "dwarf HII hot spot galaxies", "HII hot spot galaxies" or "Sargent & Searle objects".

We have used surface photometry in order to study the morphology and structural properties of HII galaxies. In Section 2, we first present the data sample. In § 3, we present our results based on the analysis of the CCD images, as well as structural aspects based on the luminosity profiles. In § 4, we discuss the results, and finally in § 5 we present some conclusions.

2 THE SAMPLE

The objects in the present study were selected from the subsample of the *Spectrophotometric Catalogue of HII Galaxies* (Terlevich et al. 1991, hereafter SCHG) used by Melnick, Terlevich & Moles (1988) in the application of HII galaxies as distance indicators. It consists of 39 HII galaxies from SCHG brighter than F(Hβ)$= 5 \times 10^{-15}$ erg cm^2 s^{-1} and with Hβ equivalent widths, W(Hβ), larger than 30 Å. The brightness criterion was adopted in order to facilitate the determination of emission line profiles, while objects with large W(Hβ) were selected to minimize age effects and contamination from an underlying stellar population. Thus, these selection criteria yield a more homogeneous sub-sample of the SCHG, namely, younger starbursts. We have reproduced the relevant data of Melnick, Terlevich & Moles (1988) in columns 1-8 in Table 1. Columns 9-12 give the results of our morphological analysis. Column 9 (prof.) describes the profile type defined in Section 3.5. Column 10 (mult.) describes whether the object shows a single (single), two (double), or more than two (multiple) knots of star formation. Column 11 (ext.) indicates whether the galaxy shows extensions or signs of distorted outer isophotes which is the primary criterion of the morphological classification given in Column 12 (type) of Table 1, and described in detail in Section 3.3. A colon next to a value in the table indicates that the classification is uncertain.

2.1 CCD images

CCD images through a broad-band V filter (λ = 5480 Å, $\Delta\lambda \approx$ 900 Å) have been obtained with the Danish 1.54-m telescope at the European Southern Observatory (ESO) in La Silla, Chile. The observations were made in the period 1986-1988. The detector was a thinned RCA CCD 512×320 ($0.47''$ per pixel) giving a total field of $4' \times 2.5'$. Exposures times were typically 1200s. Since our main aim was the study of the morphology, photometric calibration was not performed. We have nevertheless estimated magnitude zero points when data were available in the literature. Furthermore, we have not performed any correction for galactic extinction or reddening. Basic data reduction consisted of bias subtraction and flat field division, cosmic rays elimination, and sky subtraction.

3 RESULTS

In Figure 1 we present 4 panels for each object in the present study. Each page shows these panels for two objects. From top left to bottom right, the figure shows: 1) position, redshift and compiled photometric information from the NASA/IPAC Extragalactic Database (NED) plus additional photometric information from Salzer, MacAlpine & Boroson (1989a)(indicated in Figure 1 by ‡), Mazzarela & Boroson (1993)(indicated by Ш) and Telles & Terlevich (1996)(indicated by †). 2) grey scale reproduction of the CCD images. Orientation is shown for each image. The angular and physical scales are also shown on each photograph. 3) original illustrative observed spectrum of each star forming region from the SCHG. 4) circularly averaged surface brightness profiles centered on the main knot component. The magnitude zero points were determined from differential calibration using published photometry, thus they should be taken as an indicative surface brightness level only with an estimated error of at least 0.5 mag. Error bars in the profiles are 1% sky subtraction errors.

3.1 Notes on individual objects

A schematic classification of the morphology of the HII galaxies is given in the last four columns of Table 1 based on two main criteria:

multiplicity: describes whether the HII galaxy has one (single) dominant giant HII region, two (double), or more than two main knots of star formation (multiple).

Table 1. Spectroscopic data and the morphological description: (1) name as in SCHG; (2) other name; (3) redshift; (4) line width (σ) in $\mathrm{km\,s^{-1}}$; (5) Hβ flux (FHβ) in units of 10^{-13} $\mathrm{erg\,cm^2\,s^{-1}}$; (6) extinction coefficient (CHβ); (7) Hβ equivalent width in Å (WHβ) and (8) the oxygen abundance in units of 12+log(O/H). Columns (9)-(12) give the morphological description and are discussed in the text.

SCHG (1)	*other name* (2)	redshift (3)	σ (4)	FHβ (5)	CHβ (6)	WHβ (7)	O/H (8)	prof. (9)	mult. (10)	ext. (11)	type (12)
0341–407	Cam0341–4045E	0.0147	23.0	0.44	0.28	140	8.04	dd	multiple	√	I
“	Cam0341–4045W	0.0147	23.0	0.23	0.32	40					
——	Cam0357–3915	0.0741	51.1	0.47	0.17	180	7.87	d	single		II
——	Cam08–28A	0.0537	49.1	0.28	0.77	35	8.40	dd	multiple	√	I
——	Cam0840+1044	0.0115	34.0	0.10	0.39	55		bd	single	√	II:
——	Cam0840+1201	0.0305	36.5	0.48	0.52	105	7.88	d	double	√	I
——	Cam1148–2020	0.0119	33.3	1.80	0.30	230	8.01	dd	multiple	√	I
——	Cam12–39	0.0667	84.5	0.24	4.88	200	8.20	dd	double		II
1053+064	Fairall 30	0.0035	21.8	1.80	0.22	90	8.01	bd	single		II
1042+097	Fairall 2	0.0556	38.8	0.27	0.40	100	8.11	d	single		I:
——	Cam1212+1158	0.0228	34.2	0.13	0.00	60		d	single		II
0104–388	Tol0104–388	0.0211	49.0	0.30	0.39	50		bd	single		II
0127–397	Tol0127–397	0.0160	33.7	0.50	0.51	40		d	single		II
0226–390	Tol0226–390	0.0484	89.9	0.57	0.56	90	8.42	bd	single	√	I
0242–387	Tol0242–387	0.1260	134.0	0.22	0.79	60	8.23	d	single	√	I
0440–381	Tol0440–381	0.0412	39.7	0.30	0.32	35	8.31	d	single	√	I
0513–393	Tol0513–393	0.0502	33.2	0.18	0.29	145	7.90	d	single		II
0633–415	Tol0633–415	0.0177	31.8	0.45	0.35	90	8.09	dd	multiple	√	I
0645–376	Tol0645–376	0.0260	32.1	0.20	0.52	50	8.19	bd	single	√	I
1004–296	Tol1004–294S	0.0038	30.6	2.70	0.69	60	8.23	dd	double		II:
“	Tol1004–294N	0.0038	32.3	3.10	0.77	60	8.28				
1008–287	Tol1008–286	0.0141	24.0	0.30	0.52	125	8.16	bd:	multiple	√	I
1025–284	Tol1025–284	0.0321	25.2	0.30	0.48	60	8.06	dd	double	√	I:
1116–326	Tol1116–325	0.0021	12.0	0.43	0.43	275	8.31	d	single		II
1147–283	Tol1147–283	0.0064	18.9	0.24	0.47	45	7.90	d	multiple:		II
1214–277	Tol1214–277	0.0257	27.6	0.30	0.29	230	7.58	bd	single	√	I
1324–276	Tol1324–276	0.0064	33.4	0.87	0.35	115	8.20	dd	multiple	√	II:
1334–326	Tol1334–326	0.0125	16.4	0.30	0.22	265	8.00	dd	multiple	√	I
1345–421	Tol1345–420	0.0082	21.6	0.38	0.26	70	8.07	d:	single		II
——	Tol1406–174	0.0338	23.9	0.10	0.36	50		d	single		II
1924–416	Tol1924–416	0.0093	29.9	3.83	0.17	100	7.90	dd	double	√	I
2138–405	Tol2138–405	0.0578	55.5	0.33	0.25	120	7.71	dd	double	√	I
2326–405	Tol2326–405	0.0505	34.5	0.14	0.22	80	8.03	bd	double	√	I
0142+046	UM133	0.0094	17.2	0.32	0.43	65	7.64	bd:	multiple	√	II:
0131+007	UM336	0.0197	16.7	0.08	0.06	40		bd	single		II
1134+010	UM439E	0.0039	19.7	0.48	0.60	60	8.05	dd	multiple		II:
1139+006	UM448	0.0182	40.8	2.20	0.79	45	8.36	bd	double	√	I
1147–002	UM455	0.0124	20.6	0.09	0.26	55	7.84	d	single		II
1148–020	UM461A	0.0031	14.5	0.70	0.40	155	7.74	dd	double		II
1150–021	UM462A	0.0031	18.5	0.75	0.38	75	7.98	dd	double		II
“	UM462B	0.0031	18.9	1.30	0.38	90	7.79				
0553+034	IIZw40	0.0028	35.2	1.90	1.00	170	8.13	bd	double	√	I

Figure 1. Basic morphological and spectroscopic illustration for 39 HII galaxies in the present sample. Sets of panels for two objects are shown in each page. For each object we show typically 4 panels: From top left to bottom right: 1) position, redshift and compiled photometric information from NED and references therein. When available, we also include additional photometric information from Salzer, MacAlpine & Boroson (1989a)(indicated in the figure by ‡), Mazzarela & Boroson (1993)(indicated by II) and Telles & Terlevich (1996)(indicated by †). 2) scanned photographs of the CCD images. Orientation is shown for each image. The angular and physical scales are shown on each photograph. 3) original observed spectrum of the star forming region from the SCHG. 4) circularly averaged surface brightness profiles, centered on the main knot component. The magnitude zero points were determined from differential calibration using published photometry. They have not been derived from absolute calibration of the present work, thus it should be taken as an indicative surface brightness level only, and with an estimated error of at least 0.5 mag. No correction for galactic extinction or reddening has been applied. Error bars in the profiles are 1% sky subtraction errors.

outer structure: denotes the presence or absence of distorted, irregular extensions, fans or tails beyond the star forming regions.

The results of these two morphological description criteria are given in columns 10 (mult) and 11 (ext) in Table 1, respectively. Some additional notes on individual objects are given below:

SCHG 0341–407 [Cam 0341–4045] Double system; signs of multiplicity can be seen in the West knot of star formation. The faint extension on the NW direction may be all part of the same tail-like structure. This object has signs of extensions and possible merger.

Cam 0357–3915 Single; very compact; stellar object.

Cam 08–28 This Markarian object of high luminosity ($M_V \sim -22$) is in no sense a dwarf system. It has multiple structure and very irregular shape with clear signs of tails of faint surface brightness emanating from the main body to the North and South; one of the extreme examples in this sample of a possible merging system.

Cam 0840+1044 Faint extension in the E direction but no sign of interaction. This object is 2 arcminutes South from a bright foreground SBdm galaxy and close to a bright star in E.

Cam 0840+1200 L-shaped outer isophotes; irregular inner structures possibly due to multiple regions of star formation; likely to be product of a merger.

Cam 1148–2020 Multiple; main burst knot lies in the center surrounded by a ring of 3 or 4 other regions; extended outer isophotes.

Cam12–39 Compact double system; no signs of extensions.

SCHG 1053+064 [Fairall 30] Intrinsically very compact single system at low redshift with no sign of extensions; very close to bright star to West.

SCHG 1042+097 [Fairall 2] Possible unresolved double system; indication of outer faint irregular extension to W and E. It would probably show more disturbed morphology if it were at a lower redshift.

Cam1212+1158 Single; regular isophotes.

SCHG 0104–388 [Tololo 0104–388] Single and compact; close to a foreground spiral galaxy.

SCHG 0127–397 [Tololo 0127–397] Single and compact.

SCHG 0226–390 [Tololo 0226–390] Single; faint extensions from the center to the East.

SCHG 0242–387 [Tololo 0242–387] Sign of a possible tail (more visible in the CCD image) to the East at very faint surface brightness level. This object is the highest redshift galaxy in the sample. It is a member of a small group of galaxies at Z=0.126.

SCHG 0440–381 [Tololo 0440–381] Single knot; possibly unresolved double system; faint blob emanating at the South-East direction.

SCHG 0513–393 [Tololo 0513–393] Single object (southern most object in this photograph); regular shape; no sign of interaction.

SCHG 0633–415 [Tololo 0633–415] Spectacular peculiar galaxy at low redshift; very irregular morphology; bright; streamer westwards; interacting system. Most of the [OIII] emission comes from the main knot in the eastern component. Very faint line emission is also seen the western component in the narrow band [OIII] image.

SCHG 0645–376 [Tololo 0645–376] The main body is of regular shape with its burst located in the center, but faint extensions are seen to the East and to the West.

SCHG 1004–296 [Tololo 1004–294] Bright low redshift galaxy in cluster; regular outer isophotes; double knots; amorphous galaxy.

SCHG 1008–287 [Tololo 1008–286] Irregular; interacting system; two main regions of star formation embedded in common irregular envelope and bridged by faint extensions as revealed in the [OIII] image.

SCHG 1025–284 [Tololo 1025–284] Double system embedded in common envelope.

SCHG 1116–326 [Tololo 1116–325] Very compact object at low redshift.

SCHG 1147–283 [Tololo 1147–283] Single amorphous object at low galactic latitude; knots to the East may be stars superposed on the galaxy image.

SCHG 1214–277 [Tololo 1214–277] Single knot object with extensions along the North-South direction; possible close projected companion at 20 arcseconds to the South.

SCHG 1324–276 [Tololo 1324–276] Multiple knots at low redshift; in cluster; signs of faint extension along the main body; foreground bright star superposed on the South-East end.

SCHG 1334–326 [Tololo 1334–326] Multiple system of 4 knots at the centre; the most intense knot being the South West condensation; long fan emanating from the main body to the South direction only; object in cluster; bright star $\approx$ 1 arcminute to the North-West direction. Object is at low galactic latitude.

SCHG 1345–421 [Tololo 1345–420] Single object with regular outer isophotes (poor image quality).

Tololo 1406–174 Single very compact stellar object.

SCHG 1924–416 [Tololo 1924–416] Star on South-East; Multiple knots; almost triangle outer isophotes; The central region of this HII galaxy is irregular and knotty.

SCHG 2138–405 [Tololo 2138–405] Peculiar system in interaction; two distinct components. The main line emitting region is in the North while the South component has an amorphous structure. The line emitting region (North) seems to be double or of multiple knots.

SCHG 2326–405 [Tololo 2326–405] Extended cometary-like object with the main burst at its "head" at eastern-end of the elongated body; bright star at SE.

SCHG 0142+046 [UM 133] Cometary-like or Magellanic-

like object with main burst at the far South end embedded in a rather regular elongated envelope; possible multiple knots along the apparent "bar"; no evidence of interaction. This object is at low redshift. It would probably be characterized as a single object with a fuzz if it were at a larger distance.

SCHG 0131+007 [UM 336] Single object with regular outer isophotes. At a moderate redshift this object is not very compact resembling more objects with amorphous structure.

SCHG 0134–010 [UM 439] Low redshift multiple object. Main burst is in the South end; faint extensions along the main body; bright star 1.5 arcminutes to South-East.

SCHG 1139+006 [UM 448] High spatial resolution imaging of this object (Telles & Terlevich 1996) has shown double internal structure of spiral-like shape. This is a peculiar object with a visible fan, emanating directly from the main burst extending at least 2 arcminutes to the South-West .

SCHG 1147–002 [UM 455] is an elliptical shape object with the line emission region off-center. It may be an unresolved double; bright star ≈ 1.5 arcminutes to the North-East; in cluster; uncatalogued galaxy at 20 arcseconds to the East with no line emission.

SCHG 1148–020 [UM 461] Nearby double system. The main knot in the North is of much larger luminosity than the secondary one. At at moderate redshift this object would look very compact. The outer isophotes are regular despite the inner double structure being off-center.

SCHG 1150–021 [UM 462] Nearby double system. As opposed to UM 461 which is a close companion in the group, this object has the inner double structure in the center in relation with the outer regular isophotes.

SCHG 0553+034 [II Zw 40] This is a low redshift object with compact core and fan jets (South) and (South-East). This object has two clear different components which may represent a merging system. At moderate redshift its small linear size would likely hide these features. Despite its very low galactic latitude this HII galaxy has been targeted for various different studies in the literature. Recent work using HST observations by Vacca (1994) reveals that the main burst is split into smaller ionizing regions which are unresolved in ground-based observations.

3.2 General notes on morphology

Some additional general remarks can be made about the present sample:

• Objects described to have a single giant HII region usually have their burst at the center (Cam0357-3915, SCHG 1053+064, Cam1212+1158, SCHG 0104–388, SCHG 0226–390, SCHG 0242–387, SCHG 0513–393, SCHG 0645–376, SCHG 1116–326, SCHG 1345–420, SCHG 1406–174, SCHG 0131+007).

• A few objects have "pear-like" shapes (Cam 0840+1044, SCHG 1042+097, SCHG 0440–381, SCHG 1147–002). These have been classified as single systems with burst off-center. However, they can be double systems where the main knot outshines the secondary. For example, SCHG 1147–002 (UM 461) is a compact object with a double burst which would resemble a "pear-like" object, had it been located at a larger redshift.

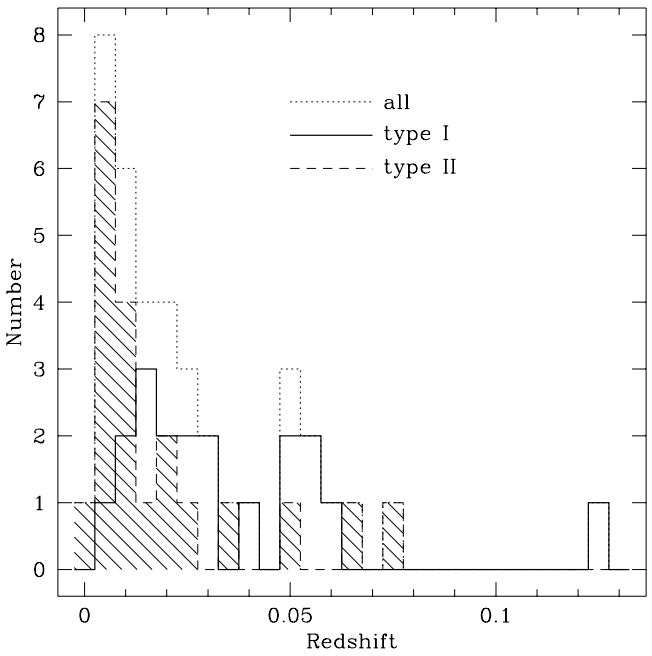

Figure 2. Redshift Distribution for Type I and Type II HII galaxies.

• Systems which appear to be double at a moderate redshift may split the two main bursts into smaller components as in the nearby example of SCHG 1324–276.

• None of the galaxies in this sample can be classified as a classical "starburst galaxy", i.e. a nuclear burst on an otherwise normal spiral galaxy. Typical HII galaxies do not show spiral structure.

3.3 A classification scheme for HII galaxies

When studying the morphological properties of HII galaxies, it is important to bear in mind that, although all contain at least one giant region of star formation (whether centered on the nucleus or not), this class presents a wide variety of morphologies. They are, in fact, a very inhomogeneous morphological class of galaxies where the common property is the dominant giant HII region. The results, presented in the last columns of Table 1 and described in more details in the previous section reveal that the presence of an extended component or possible underlying galaxy is evident in about half of these objects for which CCD images have been obtained. We also find that some of these objects show possible features of interacting or merging systems (wisps, tidal tails or irregular fuzzy extensions). More than one giant knot of star formation seems to be a common feature, although, this seems unrelated to whether the object is apparently interacting or isolated. About one third of the galaxies in the sample are actually single stellar-like objects with no evidence for extensions or fuzz.

On the basis of the shape of the *outer isophotes*, HII galaxies can be segregated in two broad groups:

Type I objects have disturbed morphologies and irregular outer isophotes, fuzz or tails.
Type II objects are symmetric and regular objects, regardless of the multiplicity of the starburst region (i.e. their internal structure).

An indication of the possible existence of these two morphological types of HII galaxies was already preliminarily reported in Telles & Terlevich (1994).

Clearly, the perception of the morphology depends on redshift. Individual star-forming regions within the galaxies may only be resolved for nearby brighter objects, while morphological details of systems at larger redshifts (z > 0.02) may be smeared out rendering the galaxies with a smoother compact appearance. HII galaxies at larger redshift which still show morphological details will be high luminosity systems that may belong to a possibly more disturbed class of starburst galaxies. These are not dwarfs. On the other hand, although small morphological features would be naturally better visible for galaxies at low redshift the distribution of redshifts shown in figure 2 shows that these Type II HII galaxies are mostly low redshift galaxies. Therefore, the fact that we do not see faint detailed structures in these low redshift, bright, low luminosity systems is not a resolution effect. Objects which are single and compact with no sign of extended envelope or tidal tails at low redshift, such as SCHG 1053+064, Cam1212+1158, SCHG 0104–388, SCHG 0127–397, SCHG 1116–326, SCHG 1345–421, Tol 1406–174 and SCHG 0131+007 are of particular interest. They may be truly young galaxies (in the sense of being experiencing their first major star formation episode) at low redshift. Thus, these objects can provide us with an insight on a era which was marked by the formation and early evolution of the present luminous galaxies.

3.4 The burst and galaxy sizes

As mentioned by Djorgovski & Davis (1987) it is difficult to define a radial scale. In principle we would need a radial scale independent from the magnitude and surface brightness calibration, which means that an isophotal radius is not ideal. However, we can use a radial scale derived from the surface brightness profiles, although we do not know the exact form of these profiles for these bursts of star formation. Therefore, the derived relations may at best be indicative of global rather than central properties of these galaxies.

We have measured the sizes of the star forming regions in the galaxies as well as the half-light radius of HII galaxies from the un-calibrated CCD images in the V band. Seeing measurements ($FWHM_*$) were obtained from Gaussian fits to the point spread function from stars in each field and are listed in column 3 of Table 2. Burst diameters (HII in arcseconds) listed in column 4 of Table 2 are FWHM of the circular brightness profiles centered on the peak intensity of the burst region of the galaxy. This method, although rather crude, provides us with a systematic estimate of the *total* physical size of the ionizing cluster that is adequate to the statistical approach to study the scaling laws governing the structural properties of HII galaxies (Telles & Terlevich 1993). In what follows, we have applied an approximate seeing correction

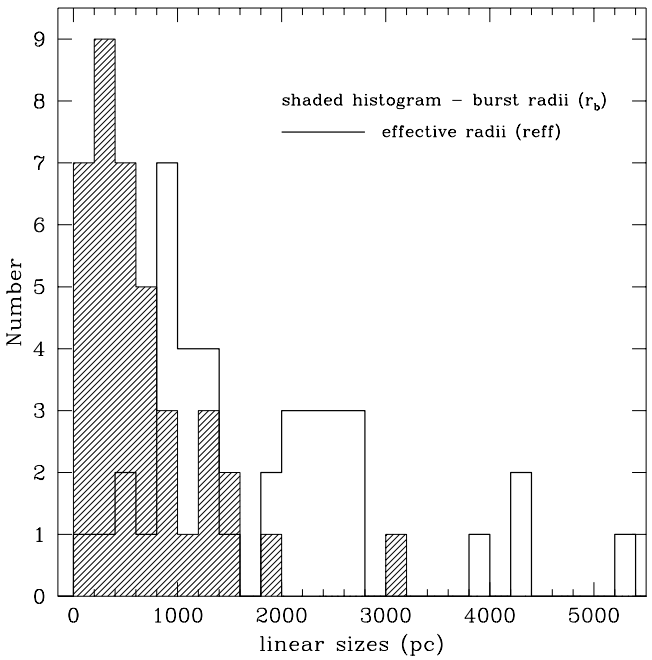

Figure 3. Distribution of linear radii of the bursts of star formation in HII galaxies (hatched histograms). The thick line histograms show the effective radii of the HII galaxies in the V filter from their luminosity curves of growth.

to the final burst sizes ($D_0^2 = FWHM_{\rm HII}^2 - FWHM_*^2$). The results are shown in columns 6 and 7 in arcseconds and in parsec†, respectively. It is important to bear in mind that for barely resolved compact regions with angular sizes of the order of the seeing disk the size estimates may represent upper limits only. This is illustrated in column 5 by the ratio of the burst size measurement to the seeing ($FWHM_{\rm HII}/FWHM_*$). Effective diameters (D_{eff} in arcseconds and in parsec) in columns 8 & 9 are the true half light diameters of the whole HII galaxy centered on the peak luminosity (main burst) measured directly from the synthetic circular aperture luminosity curve of growth for each object obtained from star-free, sky subtracted frames.

Figure 3 presents the distribution of physical sizes (burst radii, r_b) of the bursts of star formation as shaded histograms and the distribution of effective radii ($r_{\rm eff}$) of HII galaxies. From this, one can see that star forming regions have typical sizes of hundreds of parsec and there is a significant cut off above these values. It is worth noting that these sizes are representative of the *total* size of the ionizing cluster. True *core* sizes of the ionizing cluster will be far smaller. If one takes 30 Doradus, the most spectacular example of a nearby giant HII region in the LMC, and compare the ratio of sizes of its ionized region to its ionizing cluster resolved by the Hubble Space Telescope (HST) (Walborn 1991), one would expect equivalent core sizes of the ionizing stellar clusters of the gigantic HII regions in galaxies to be at least 100 times smaller than their ionized regions, thus of the order of a few parsec. They will remain completely

† $H_0 = 50$ km s^{-1} Mpc^{-1} is used throughout this paper.

unresolved and, if they are like 30 Dor, most of the ionizing luminosity will be produced in this small region.

3.5 Luminosity Profiles

We have adopted the simplest procedure of fitting *circularly* averaged radial profiles to represent the light distribution in the isophotes of HII galaxies. Fitting ellipses to the irregular isophotes of HII galaxies does not produce any additional information about the true structure of one particular galaxy. In either case the resulting profiles are similar. Figure 1 shows the derived luminosity profiles, from star-free frames, for each HII galaxy in our present sample represented as surface magnitude $\mu(r)$ plotted against radius r. In this representation an exponential profile is a straight line.

Figure 4 shows the three main types of overall light profiles found among HII galaxies. The power law profile (solid line) is mostly found in galaxies with long extensions. These resemble, somewhat, the two-component profiles such as bulge + disk profiles typical of bright early type spiral galaxies. They trace light to larger angular sizes [e.g. SCHG 0633–415, SCHG 2326–405, SCHG 0553+034 (II Zw 40)]. Exponential profiles (dotted lines) typically describe the more compact, small angular size objects and are heavily affected by the point spread function (e.g. Cam 0357–3915, SCHG 1042+097, SCHG 1116–326). Platform profiles (dashed line) are found for galaxies with more than one main knot [e.g. SCHG 0341–407, SCHG 1004–296 and SCHG 1134+010 (UM 439)].

We will label the three typical types of profiles as follows:

d A single exponential fit represents well the whole range of radii of the profile.
dd Double profile with a "platform" due to the double morphology. An exponential law is well fitted to the outer regions.
bd a steep bright central region and outer disk-like component. No attempt is made to perform a bulge-disk like decomposition because of the unknown relation of the light in the burst region with the mass density and the unknown analytical form of the light profile in the inner region. The exponential fit represents well the outer component only.

The results of this classification scheme for the light profiles of HII galaxies are shown in column 9 of Table 1.

A natural further step in the analysis of the luminosity profiles of HII galaxies is to fit the profiles with known scaling laws. The most common scaling laws are: exponential $\mu(r) \propto r$ (Freeman 1970); $\mu(r) \propto r^{1/4}$ (de Vaucouleurs 1948); $\mu(r) \propto log(r)$ (Bahcall 1977); $I(r) = I_0(1 + \frac{r^2}{r_0^2})^{-1}$ (Hubble 1930). Although these photometric laws describe the luminosity profiles of normal galaxies they should actually not be used as morphology descriptors; an exponential profile does not imply a disky system unless a disk is clearly seen or there is other indication that this may be the case. Surface photometry alone is helpful but not sufficient to determine the spatial structure of a particular dwarf whether it may be spheroidal or disk-like. We have studied which of these common scaling laws best represents the overall shape of each HII galaxy. The main conclusion from this study

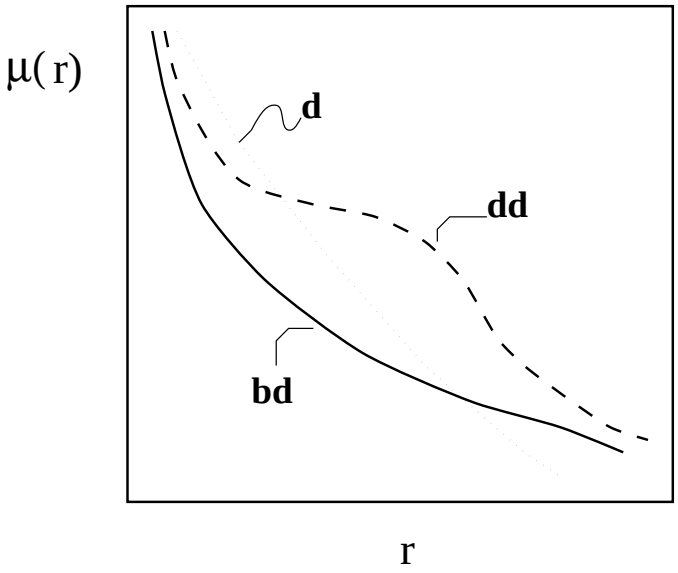

Figure 4. Profile types.

is that *outer parts* of all three types of luminosity profiles of HII galaxies are well described by an exponential scaling law (i.e. exponential fits have the lowest standard deviation when the outer profiles are fitted to the same radial range). These findings for HII galaxies agree with those of Vader & Chaboyer (1994) who find a general predominance of exponential profiles among dwarf of various types although composite profile and early type $r^{1/4}$ similar to giant ellipticals do occur in some cases.

Therefore, the structural parameters derived from the exponential fits (i.e. scale length r_0 and central surface brightness μ_0) to the extensions may well represent the structural properties of the underlying galaxy in HII galaxies. In Table 3 we present the results of such exponential fits for our present sample. Unfortunately, we do not have absolute calibration and we are able to give approximate central surface brightness values for only $\sim$ 40 % of the present sample. We also caution that no reddening correction has been applied. One may wish to compare the results of the structural parameters of HII galaxies directly with the properties of other known types of dwarfs such as dE's, dIrr's or other low surface brightness galaxies. A comparison may help give us some insight on the origin of the HII galaxies and the relation among all dwarf galaxies. However, the large uncertainty in the zero point of the few galaxies for which we have differential calibration prevent us from performing such comparison until more an better quality data are available.

4 DISCUSSION

Figure 5 shows the distributions of the intrinsic properties of HII galaxies segregated in Type I HII galaxies (solid line histograms) and Type II HII galaxies (shaded histograms). Also shown, as dotted lines, are the histograms for all galaxies in the sample. Table 4 summarizes the main statistical parameters from these distributions. We have checked the trends shown in figure 5 by performing a Kolmogorov-

Table 2. Size measurements. $FWHM_*$ is the FWHM seeing from a Gaussian fit to a stellar image in the CCD field. $FWHM_{\rm HII}$ are the main burst sizes in arcseconds. D_0 are the burst sizes corrected by the seeing as described in the text. D_{eff} are the half-total light diameters from the luminosity curves of growth.

SCHG	*other name*	$FWHM_*$	$FWHM_{\rm HII}$	$\frac{FWHM_{\rm HII}}{FWHM_*}$	D_0		D_{eff}	
		(")	(")		(")	(pc)	(")	(pc)
0341–407	Cam0341–4045E	1.47	2.31	1.57	1.79	764	18.51	7915
——	Cam0357–3915	1.53	2.03	1.33	1.34	2886	2.17	4670
——	Cam08–28A	1.28	2.69	2.11	2.37	3706	6.78	10595
——	Cam0840+1044	1.32	2.11	1.60	1.65	551	7.16	2395
——	Cam0840+1201	1.26	2.01	1.60	1.57	1393	5.18	4597
——	Cam1148–2020	1.64	2.75	1.68	2.20	763	15.64	5413
——	Cam12–39	1.51	1.94	1.29	1.22	2372	2.45	4752
1053+064	Fairall 30	1.64	2.42	1.48	1.78	181	6.69	681
1042+097	Fairall 2	1.32	2.18	1.65	1.73	2799	3.25	5256
——	Cam1212+1158	1.36	1.95	1.43	1.40	926	2.62	1737
0104–388	Tol0104–388	1.13	2.05	1.82	1.71	1051	2.75	1688
0127–397	Tol0127–397	1.63	2.62	1.61	2.05	955	5.18	2411
0226–390	Tol0226–390	1.13	1.76	1.56	1.35	1899	2.73	3846
0242–387	Tol0242–387	1.28	2.09	1.63	1.65	6050	2.30	8425
0440–381	Tol0440–381	1.23	2.92	2.37	2.65	3178	3.37	4042
0513–393	Tol0513–393	1.39	1.84	1.32	1.20	1747	2.17	3164
0633–415	Tol0633–415	1.41	2.25	1.59	1.75	902	7.54	3880
0645–376	Tol0645–376	1.34	2.36	1.77	1.95	1475	6.46	4888
1004–296	Tol1004–294S	1.19	2.14	1.79	1.78	196	18.37	2031
1008–287	Tol1008–286	1.20	1.85	1.54	1.40	575	12.06	4946
1025–284	Tol1025–284	1.19	1.89	1.60	1.48	1378	5.65	5278
1116–326	Tol1116–325	1.43	2.21	1.55	1.69	103	2.49	152
1147–283	Tol1147–283	1.39	3.80	2.73	3.53	658	9.70	1806
1214–277	Tol1214–277	1.14	1.74	1.54	1.32	989	2.25	1683
1324–276	Tol1324–276	1.11	2.16	1.94	1.85	344	13.66	2543
1334–326	Tol1334–326	1.50	2.12	1.42	1.50	545	7.16	2603
1345–421	Tol1345–420	1.58	3.75	2.38	3.41	812	10.93	2607
——	Tol1406–174	1.41	2.03	1.43	1.45	1427	2.15	2112
1924–416	Tol1924–416	1.52	4.89	3.22	4.65	1258	6.03	1631
2138–405	Tol2138–405	1.11	1.98	1.78	1.64	2761	2.57	4324
2326–405	Tol2326–405	1.13	1.76	1.56	1.35	1981	2.83	4151
0142+046	UM133	1.62	3.28	2.03	2.86	781	32.03	8758
0131+007	UM336	1.10	1.98	1.79	1.64	941	3.81	2181
1134+010	UM439	1.38	1.96	1.42	1.39	158	15.64	1774
1139+006	UM448	1.36	4.94	3.64	4.75	2515	9.42	4987
1147–002	UM455	1.75	2.36	1.35	1.59	572	5.12	1845
1148–020	UM461A	1.39	3.52	2.53	3.23	291	9.24	833
1150–021	UM462A	1.49	7.19	4.83	7.04	635	13.80	1244
0553+034	IIZw40	1.45	2.76	1.90	2.35	191	12.25	997

Table 4. Statistical results for the distributions of figure 5a-d. The mean and median of the distribution are given for Type I and Type II HII galaxies separately. The last column gives the probability P that the distributions of these spectroscopic properties are drawn from the same distribution function (see text for details).

	Type I		Type II		
	Mean	Median	Mean	Median	K-S test
$\log L(H\beta)$ (erg s^{-1})	41.67±0.60	41.41±0.53	40.64±0.84	40.30±0.48	P = 0.001
σ (km s^{-1})	40.0±24.2	32.9±6.6	28.7±15.6	23.1±7.3	P = 0.02
W(Hβ) (Å)	112±68	100±40	94±64	65±45	P = 0.18
$12 + \log$(O/H)	8.07±0.21	8.09±0.09	7.99±0.19	8.01 ±0.16	P = 0.51

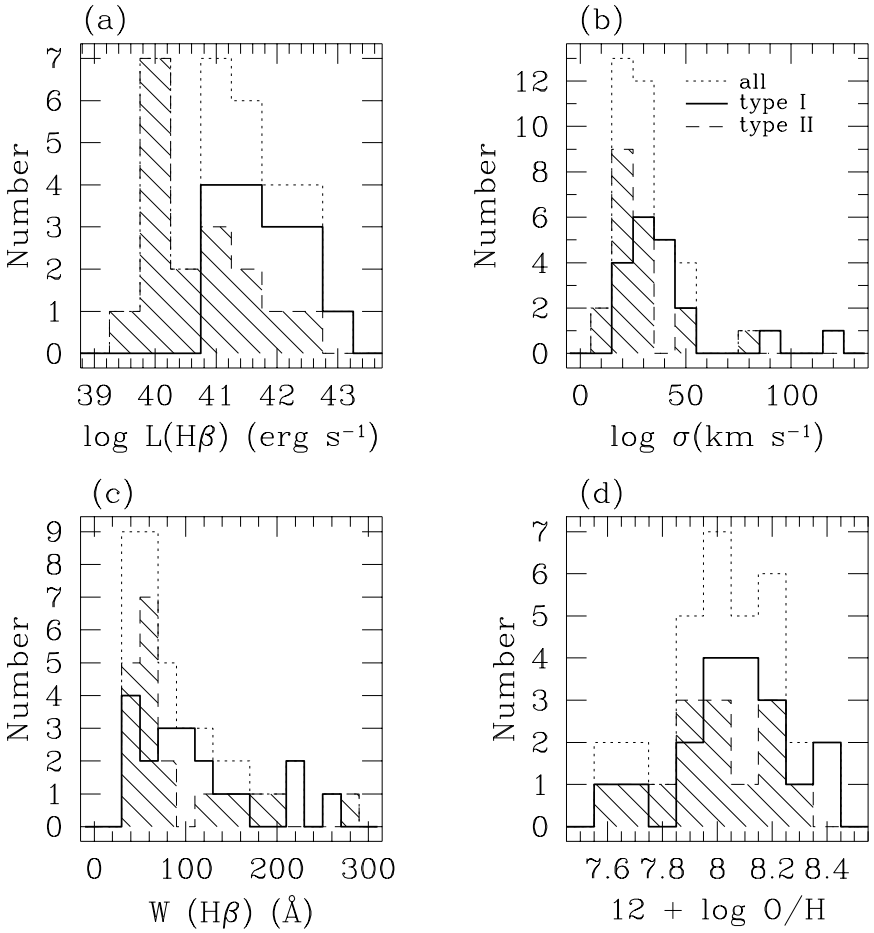

Figure 5. Histogram of the spectroscopic properties segregated in Type I HII galaxies and Type II HII galaxies. Dotted lines show the distributions for the whole sample. Solid line histograms are Type I HII galaxies, while short-dashed hatched histograms show Type II HII galaxies.

Smirnov test to the unbinned distributions in order to assess statistically the differences of the spectroscopic data for Type I and Type II HII galaxies. The low values of the significance level ($P \leq 0.02$) disproves that the distributions of L(Hβ) and σ can be drawn from the same distribution function. However, the high values of the significance level ($P > 0.1$) for the distributions of W(Hβ) and O/H indicate that the data are consistent with them being drawn from a single distribution function. These results show that HII galaxies with signs of disturbed morphologies (Type I) tend to be more luminous than Type II objects. It can also be seen that Type I also tend to have larger velocity dispersion (σ) in the line emission regions in agreement with the well known correlation between L(Hβ) and σ (Terlevich & Melnick 1981; Melnick, Terlevich & Moles 1988). The metal abundance and W(Hβ) distributions seem to overlap for both types of HII galaxy. However, the morphological disturbances of Type I HII galaxies do not seem to be of tidal origin. HII galaxies are not associated with bright companions, they are mostly isolated and tend to populate low density environments and are weakly clustered (Telles & Terlevich 1995; Vilchez 1995; Rosenberg, Salzer & Moody 1994).

It is interesting to point out that other types of dwarf galaxies have been found to show distinct systematic structural properties at both ends of the luminosity distribution (Binggeli & Cameron 1991, Binggeli 1994, Ferguson & Binggeli 1994). Binggeli & Cameron (1991) have found that the break in the systematic photometric properties in their sample of ~ 200 early-type dwarfs in the Virgo cluster lies at $M_B \approx -16$ to -17. They suggested that this may be caused by a transition in the internal kinematics of the systems from disky or rotationally supported systems to spheroidal systems. They also suspect a connection with the ratio of visible to dark matter; fainter galaxies being more dark matter dominated. The question that then arises is whether there is indeed a real break in physical properties of all dwarf galaxies at that luminosity. If so, what is the relation and underlying causes between the break at the photometric properties for the dwarfs in Virgo and the apparent break in the morphological properties of HII galaxies? In any case, our results seem to suggest a strong relation between morphology and luminosity.

Apart from the photometric evolution of the stellar population in HII galaxies, because of the mass loss from stellar winds and supernova ejecta and its short dynamical time scale, dynamical evolution will affect the system in less than

Table 3. Structural parameters from exponential fits: μ_0 is the extrapolated central surface brightness and r_0 is the scale length (in arcseconds) of an exponential fit to the *extensions* of the luminosity profiles.

SCHG	*other name*	μ_0	r_0
0341–407	Cam0341–4045		10.4
——	Cam0357–3915		0.6
——	Cam08–28A	22.1	4.9
——	Cam0840+1044	23.2	3.4
——	Cam0840+1201		1.6
——	Cam1148–2020		7.4
——	Cam12–39		1.3
1053+064	Fairall 30		2.4
1042+097	Fairall 2		1.0
——	Cam1212+1158	19.8	1.0
0104–388	Tol0104–388		1.7
0127–397	Tol0127–397		3.1
0226–390	Tol0226–390		1.8
0242–387	Tol0242–387		0.9
0440–381	Tol0440–381		1.1
0513–393	Tol0513–393		1.0
0633–415	Tol0633–415	25.2	15.0
0645–376	Tol0645–376		5.6
1004–296	Tol1004–294	19.9	7.5
1008–287	Tol1008–286		3.8
1025–284	Tol1025–284		1.8
1116–326	Tol1116–325		0.7
1147–283	Tol1147–283	21.4	4.1
1214–277	Tol1214–277		3.4
1324–276	Tol1324–276	20.2	5.4
1334–326	Tol1334–326	19.3	2.0
1345–421	Tol1345–420		2.2
——	Tol1406–174		0.5
1924–416	Tol1924–416	17.3	5.9
2138–405	Tol2138–405		1.4
2326–405	Tol2326–405		4.9
0142+046	UM133	23.1	14.1
0131+007	UM336	22.6	2.4
1134+010	UM439	19.5	3.9
1139+006	UM448	23.7	14.0
1147–002	UM455	20.3	1.8
1148–020	UM461	20.8	3.0
1150–021	UM462	19.5	3.8
0553+034	IIZw40	22.2	10.0

a Hubble time (Terlevich 1994). We can predict the trend of the effect of mass loss in the dynamical evolution of the stellar cluster. If the removal is slow compared to the crossing time of the system t_{ff}, then the system obeys an adiabatic invariant (Dekel & Silk 1986, Terlevich 1994 and references therein), and the "bloating" of the stellar system will be proportional to the mass loss. For the system to remain bounded throughout its evolution, the increase in size should be accompanied by a corresponding decrease in velocity dispersion:

$$\frac{r}{r_0} = \frac{\mathcal{M}_0}{\mathcal{M}} = \frac{\sigma_0}{\sigma}$$

where r is the size of the system, $\mathcal{M}$ is its total mass and σ is the velocity dispersion. During the evolution the total mass lost by a "normal" IMF population is in the range of 20% - 40%, considering that all ejecta leave the system.

Figure 6 shows the [R – σ] relation for our sample of

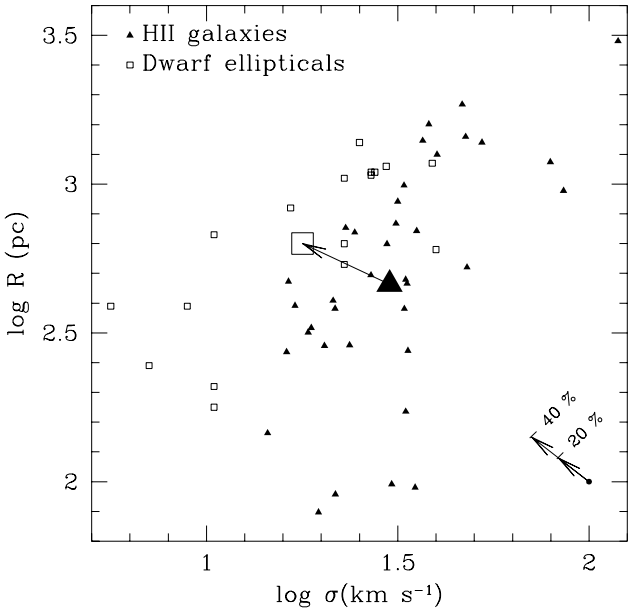

Figure 6. The Radius vs. σ relations for dEs and HII galaxies. R corresponds to R_b ($D_0/2$ from Table 2) for HII galaxies. The big symbols represent the mean locus of the HII galaxies (big solid triangle) and the mean locus of the dwarf elliptical galaxies in the diagram (big open square).

HII galaxies (solid triangles) and compares it with sample of dwarf elliptical galaxies (open squares) from Peterson & Caldwell (1993, and references therein). The big symbols represent the mean locus of the HII galaxies (big solid triangle) and the mean locus of the dwarf elliptical galaxies in the diagram (big open square). The arrow connecting the big symbols is the observed shift from the HII galaxies to the dwarf elliptical galaxies. This trend, namely that dwarf ellipticals are typically slightly larger and with lower velocity dispersion than HII galaxies, is compatible with the expectation if the stellar population in HII galaxies evolve dynamically into dwarf elliptical galaxies. In addition, the magnitude of the observed shift is in good agreement with the estimated dynamical evolution due to mass loss by a "normal" IMF population ($\Delta\mathcal{M}/\mathcal{M}, \sim 20\% - 40\%$), represented in the figure by the arrows in the right lower corner. The similarity of the parametric relations of "aged" HII galaxies with those of other dwarf galaxies (Telles & Terlevich 1993), together with the indication of a possible dynamical evolution of HII galaxies into dwarf ellipticals, may be suggestive of a close kinship among these dwarfs.

5 CONCLUSIONS

The morphological and structural properties of HII galaxies are studied in this paper. The main conclusions of this study are:

• HII galaxies can be classified within two broad morphological types:

Type I irregular systems with signs of distorted outer isophotes, tails, wisps, fans, etc.

Type II regular and compact systems with symmetric morphology.

Type I's were found to have higher luminosities and velocity dispersions than Type II's, while the equivalent widths of Hβ and oxygen abundances of the two types are roughly similar. This seems to indicate that the starbursts may have been triggered by different mechanisms in the two classes of objects.

- We find three main types of light profiles in HII galaxies. The profile types *qualitatively* relate to the overall morphology of the galaxies. The outer parts of the luminosity profiles of HII galaxies are well represented by an exponential scaling law. This will allow a direct comparison of the structural parameters (scale length and central surface brightness) with other types of dwarf galaxies and will lead us to derive important structural properties of the underlying systems once calibrated images are obtained.
- While the burst sizes of HII galaxies are of the order of hundreds of parsec, the "true" core radii of HII galaxies are basically unresolved and probably only few parsecs across. Yet, most of the ionizing luminosity produced may be coming from these very small regions.
- The similar trends of dynamically "aged" HII galaxies, and their relative positions in the [R – σ] diagram support the hypothesis of a possible evolutionary link between the two types of galaxy. If this is the case, dEs could be the descendants of HII galaxies.

ACKNOWLEDGMENTS

ET acknowledges his grant from CNPq/Brazil. We especially thank Richard Sword for his art work in this paper.

REFERENCES

Bahcall N.A., 1977, Ann. Rev. Astr. Astrophys. , 15, 505
Binggeli B., 1994, in "ESO/OHP Workshop on Dwarf Galaxies", eds. G.Meylan and P.Prugniel, ESO, Garching bei München, p. 13
Binggeli B. & Cameron L.M., 1991, A&A, 252, 27
Bothun G.D., Mould J.R., Caldwell N. & Macgillivray H.T., 1986, AJ, 92, 1007
Davies J.I. & Phillipps S., 1988, MNRAS, 233, 553
Dekel A. & Silk J., 1986, ApJ, 303, 39
Djorgovski S. & Davis M., 1987, ApJ, 313, 59
Drinkwater M. & Hardy E., 1991, AJ, 101, 94
Ferguson H.C. & Binggeli B., 1994, Astron. Astrophys. Rev. , 6, 67
Freeman K.C., 1970, ApJ, 160, 811
Hubble E.P., 1930, ApJ, 71, 231
Kunth D., Maurogordato S. & Vigroux L., 1988, A&A, 204, 10
Loose H.H. & Thuan T.X., 1985, in "Star Forming Dwarf Galaxies", eds. D.Kunth, T.X.Thuan and J.Tran Thanh Van, editions Frontières Gif Sur Yvette, France, p. 73
Mazzarella J.M. & Boroson T.A., 1993, ApJS, 85, 27
Melnick J., 1987, in "Starburst and Galaxy Evolution", eds. T.X.Thuan, T.Montmerle & J.Tran Thanh Van, editions Frontières Gif Sur Yvette, France, p. 215
Melnick J., Terlevich R. & Eggleton P., 1985, MNRAS, 216, 255
Melnick J., Terlevich R. & Moles M., 1988, MNRAS, 235, 297
Meurer G.R., Freeman K.C. & Dopita M.A., 1992, AJ, 103, 60
Meurer G.R., Mackie G. & Carignan C., 1994, AJ, 107, 2021
Peterson R.C. & Caldwell N., 1993, AJ, 105, 1411
Rosenberg J.L., Salzer J.J. & Moody J.W., 1994, AJ, 108, 1557
Salzer J.J., MacAlpine G.M. & Boroson T.A., 1989a, ApJS, 70, 447
Salzer J.J., MacAlpine G.M. & Boroson T.A., 1989b, ApJS, 70, 480
Sargent W.L.W. & Searle L., 1970, ApJL, 162, L155
Sérsic J.L. & Donzelli C.J., 1992, Astrophys. Space Sci., 193, 87
Telles E., 1995, PhD. Thesis, Univ. of Cambridge
Telles E. & Terlevich R., 1993, Astrophys. Space Sci., 205, 49
Telles,E. & Terlevich,R., 1994, in "Violent Star formation from 30 Doradus to QSO's", ed. G.Tenorio-Tagle, Cambridge University Press, p. 202
Telles E. & Terlevich R., 1995, MNRAS, 275, 1
Telles E. & Terlevich R., 1996, MNRAS, accepted (astro-ph/9610136)
Terlevich R., 1994, in "Violent Star Formation", Tenorio-Tagle, G., ed., Cambridge Univ. Press, Cambridge, p. 329
Terlevich R. & Melnick J., 1981, MNRAS, 195, 839
Terlevich R., Melnick J., Masegosa J., Moles M. & Copetti M.V.F., 1991, A&AS, 91, 285 (SCHG)
Thuan T.X., 1983, ApJ, 268, 667
Vacca W.D., 1994, in "Violent Star Formation: From 30 Doradus to QSO's", ed. G. Tenorio-Tagle, Cambridge Univ. Press, Cambridge, p. 297
Vader J.P. & Chaboyer B., 1994, AJ, 108, 1209
de Vaucouleurs G., 1948, Ann. d'Astrophys., 11, 247
Vilchez J.M., 1995, AJ, 110, 1090
Walborn N.R., 1991, in "Massive Stars in Starbursts", eds. C. Leitherer, N.R. Walborn, T.M. Heckman & C.A. Norman, Cambridge Univ. Press, Cambridge, p. 145